General Disclaimer

One or more of the Following Statements may affect this Document

- This document has been reproduced from the best copy furnished by the organizational source. It is being released in the interest of making available as much information as possible.

- This document may contain data, which exceeds the sheet parameters. It was furnished in this condition by the organizational source and is the best copy available.

- This document may contain tone-on-tone or color graphs, charts and/or pictures, which have been reproduced in black and white.

- This document is paginated as submitted by the original source.

- Portions of this document are not fully legible due to the historical nature of some of the material. However, it is the best reproduction available from the original submission.

Effects of Structural Coupling on Mistuned Cascade Flutter and Response

Robert E. Kielb
Lewis Research Center
Cleveland, Ohio

and

Krishna Rao V. Kaza
The University of Toledo
Toledo, Ohio

NASA

EFFECTS OF STRUCTURAL COUPLING ON MISTUNED CASCADE FLUTTER AND RESPONSE

Robert E. Kielb*

National Aeronautics and Space Administration
Lewis Research Center
Cleveland, Ohio 44135

and

Krishna Rao V. Kaza†

The University of Toledo
Toledo, Ohio 43606 and

National Aeronautics and Space Administration
Lewis Research Center
Cleveland, Ohio 44135

ABSTRACT

The effects of structural coupling on mistuned cascade flutter and response are analytically investigated using an extended typical section model. Previous work using two degree of freedom per blade typical section models has included only aerodynamic coupling. The present work extends this model to include both structural and aerodynamic coupling between the blades. The model assumes that the structurally coupled system natural modes have been determined and can be represented in the form of N bending and N torsional uncoupled modes for each blade, where N is the number of blades and, hence, is only valid for blade dominated motion. The aerodynamic loads are calculated by using two-dimensional unsteady cascade theories in the subsonic and supersonic flow regimes. The results show that the addition of structural coupling can affect both the aeroelastic stability and frequency. The stability is significantly affected only when the system is mistuned. The resonant frequencies can be significantly changed by structural coupling in both tuned and mistuned systems, however, the peak response is significantly affected only in the latter.

NOMENCLATURE

$[A]$	aerodynamic matrix due to motion
(AD)	aerodynamic matrix due to wake induced flow
a	elastic axis position
b	semichord
c	chord
$[D],[D_s]$	matrices defined in Eq. (5)
$[E]$	transformation matrix
e	base for natural logarithm
$[G],[G_s]$	matrices defined in Eq. (6)
G_{Khsr}, G_{Kasr}	defined in Eq. (6)
h_{ar}	bending deflection of blade in r^{th} mode of tuned cascade
h_s	bending deflection of sth blade
I_{α_s}	mass moment of inertia of sth blade about elastic axis per unit span
i	square root of minus one, also a summation index
K_{hsr}, K_{asr}	bending and torsional stiffness of sth blade in r^{th} mode, respectively
k	reduced frequency based on semichord
L_s^m	lift due to motion of sth blade per unit span, positive up
L_s^w	lift due to wakes of sth blade per unit span, positive up
l_{hhr}, l_{har}	nondimensional lift coefficients due to bending and torsional motions, respectively, in the rth mode
l_{ahr}, l_{aar}	nondimensional moment coefficients due to bending and torsional motion, respectively, in the rth mode
l_{whr}, l_{war}	nondimensional lift and moment coefficients, respectively, due to wakes in the rth mode
M	Mach number
M_s^M	moment about the elastic axis due to motion of the sth blade per unit span, positive nose up
M_s^w	moment of sth blade per unit span about the elastic axis due to wake, positive nose up

E-1500

m_s	mass per unit span of the sth blade	ω_{hs}	$\sqrt{K_{hs}/m_s}$
N	number of blades	$\omega_{\alpha s}$	$\sqrt{K_{\alpha s}/I_{\alpha s}}$
$[P]$	matrix defined in Eq. (10)		
$[Q]$	matrix defined in Eq. (7)	ω_{hsr}	bending natural frequency, dependent on r
r	integer specifying the nodal diameter or interblade phase angle mode of the tuned rotor	$\omega_{\alpha sr}$	torsional natural frequency, dependent on r
r_{α_s}	radius of gyration of sth blade, nondimensionalized with respect to b	ω_{hr}	tuned bending frequency, dependent on r
s	integer specifying blade number, also blade ω	$\omega_{\alpha r}$	tuned torsional frequency, dependent on r
S_{α_s}	static mass moment of the sth blade per unit span about elastic axis, positive when center of gravity is aft of the elastic axis	$[\ ]^{-1}$	inverse of a matrix
t	time		
V	freestream velocity relative to the blade		
(X)	physical blade displacements		
X,Z	rectangular coodinate axes		
x_{α_s}	nondimensional static unbalance of sth blade		
(Y)	displacements in nodal diameter modes		
α_s	amplitude of torsional motion of sth blade, positive clockwise		
$\alpha_{s,id}$	torsional amplitude of each blade of the tuned rotor		
α_{ar}	amplitude of torsional deflection of a blade in the rth mode of a tuned cascade		
β_r	interblade phase angle, $2\pi r/N$		
γ	nondimensional eigenvalue, $(\omega_0/\omega)^2$		
γ_{hr}, γ_{ar}	defined in Eq. (14)		
$\gamma_{hsr}, \gamma_{asr}$	defined in Eq. (4)		
ζ_{hsr}, ζ_{asr}	damping ratios of the sth blade in bending and torsion in r^{th} mode, respectively		
μ_s	mass ratio of the sth blade		
$\bar{\mu}$	real part of eigenvalue, defined in Eq. (12)		
$\bar{\nu}$	imaginary part of eigenvalue, defined in Eq. (12)		
ζ	stagger angle		
ω	frequency		
ω_0	reference frequency		

I. INTRODUCTION

In Refs. (1) and (2) the authors have investigated the effects of mistuning on cascade flutter and response by assuming that the individual blades in the cascade are coupled only aerodynamically. A typical section model, in which each blade has two degrees of freedom, one bending and one torsional, was used. In all bladed-disc assemblies the blades are structurally coupled through the disc and often through a variety of other connecting parts such as shrouds, dampers, and lacing wires. In the case where there is only weak structural coupling between the blades (e.g., a relatively stiff disc and flexible blades), the effect of the structural coupling on individual blade frequencies is negligible and the method of analysis used in the previous publications is adequate. To handle cases where there is significant structural coupling, the typical section model must be refined. The purposes of this paper are to present such a refined model to account for structural coupling and to study its effects on cascade flutter and aeroelastic response of a mistuned bladed-disc. The work presented is limited to bladed-discs in which the motions are dominated by the blades and is based on a portion of the research described in Ref. (3).

The only known published work on mistuning including both aerodynamic and structural coupling is given in Ref. (4), in which each blade is allowed a single torsional degree of freedom and a subsonic aerodynamic theory is used to investigate flutter. In the present paper the model is capable of considering coupled bending and torsional motion and both subsonic (Ref. (5)) and supersonic (Ref. (6)) two dimensional unsteady cascade aerodynamic theories are used to investigate flutter and aeroelastic response. Since the effects of bending-torsion coupling were examined in Refs. (1) and (2), the parametric studies are limited to predominantly torsional motion with structural coupling. In addition to the references mentioned above, some other publications dealing with mistuning are (1) structural coupling without aerodynamics (Refs. (7) to (10)) and (2) flutter and response using single degree of freedom blade models with aerodynamic coupling only (Refs. (11) to (14)). Tuned systems with two degrees of freedom per blade have been considered in Refs. (15) to (20). In Ref. (21) the authors have considered a more complex beam model which is capable of representing a twisted nonuniform blade.

II. THEORY

It is well known that the natural frequencies of annular plates depend upon the number of nodal diame-

ters. In many publications (e.g., Refs. ([7]) to ([10]))
this behavior has also been shown to be true for
bladed-disc assemblies. For tuned systems each single-
blade mode, such as the first bending mode, becomes a
family of modes, one for each nodal diameter pattern.
In general, the frequencies for the first bending fam-
ily of modes can vary considerably and depend monoton-
ically on the number of nodal diameters. However, for
torsional motion the frequencies are relatively insen-
sitive to nodal diameter and do not increase monoton-
ically. For a more detailed discussion of this behav-
ior see Ref. ([3]).

In general, a complete bladed-disc model must in-
clude blade models, a disc model, and the appropriate
continuity conditions. Simpler approaches can be used
for the two limiting conditions of blade and disc dom-
inated motion. For disc dominated motion, the blades
can be considered to be lumped masses with no effect
on the system stiffness. For blade dominated motion,
the disc can be considered to be a spring support with
no effect on the system mass. This latter approach is
used herein and, hence, is only valid for blade domi-
nated motion. The authors are developing a complete
bladed-disc model which will be described in a future
publication.

The approach used in formulating the mathematical
model is to assume that the structurally coupled sys-
tem modes (in a vacuum) have been determined and can
be represented in the form of N bending and N tor-
sional uncoupled modes for each blade. That is, each
blade will appear to have 2N natural frequencies:
one bending and one torsion for each nodal diameter
pattern. This description requires that the disc (and/
or shroud ring) be a perfect body of revolution with
all of the mistuning effects lumped in the individual
blades. Since the number of nodal diameters, r, is
directly related to the interblade phase angle by

$$\beta_r = 2\pi r/N \qquad (1)$$

each interblade phase angle mode is associated with a
given nodal diameter. The parameter, β_r, is used in
the "traveling wave approach" of describing blade mo-
tion. In this approach the motion of the airfoils in
each mode of the tuned cascade is assumed to be simple
harmonic with a constant phase angle between adjacent
blades. This approach is entirely equivalent to the
"standing wave approach" in which the motion is char-
acterized by modes with nodal diameters fixed in the
disc. For further discussion of the standing and
traveling wave approaches see Ref. ([20]). To include
structural coupling, the equations of motion given in
Ref. ([2]) have to be modified to reflect the fact that
the blade frequencies in a vacuum depend on the number
of nodal diameters. This is accomplished by assuming
that only the stiffness terms are functions of the
number of nodal diameters. Hence, the natural fre-
quencies in a vacuum are given an additional subscript
to reflect this dependency. Also, the force (or mo-
ment) associated with the stiffness in the equations
of motion is assumed to be proportional to the dis-
placement in the rth nodal diameter mode, and not to
the physical blade deflection. As a result, the
stiffness terms must be multiplied by the modal dis-
placement and not the blade physical displacement.
The term "modal displacement" is used since the physi-
cal displacements are expanded in terms of the nodal
diameter modes. Also, the structural damping associa-
ted with the bending and torsional motions is also
allowed to be a function of the number of nodal
diameters.

As in Refs. ([1]) and ([2]), each blade is modeled as
a two degree of freedom oscillator in which the plung-
ing and pitching motions are inertially coupled (see

Fig. 1). Including the nodal diameter dependence de-
scribed above, the equations of motion of the sth
blade are

$$\begin{bmatrix} m_s & S_{\alpha_s} \\ S_{\alpha_s} & I_{\alpha_s} \end{bmatrix} \left\{ \begin{array}{c} \dfrac{d^2}{dt^2}\left(h_s e^{i\omega t}\right) \\ \dfrac{d^2}{dt^2}\left(\alpha_s e^{i\omega t}\right) \end{array} \right\} +$$

$$+ \sum_{r=0}^{N-1} \begin{bmatrix} (1 + 2i\zeta_{hsr})m_s\omega_{hsr}^2 & 0 \\ 0 & (1 - 2i\zeta_{\alpha sr})I_{\alpha_s}\omega_{\alpha sr}^2 \end{bmatrix}$$

$$\cdot \left\{ \begin{array}{c} h_{ar} \\ \alpha_{ar} \end{array} \right\} e^{i(\omega t + \beta_r s)} = \left\{ \begin{array}{c} -L_s^M - L_s^w \\ M_s^M + M_s^w \end{array} \right\} \qquad (2)$$

These are identical to Eq. (4) of Ref. ([2]) with the
following exceptions: the stiffness terms are now ex-
panded to include the stiffness associated with each
nodal diameter mode and the physical displacement terms
are replaced with the modal displacements. Note that
the real parts of the modal stiffnesses, K_{hsr} and
$K_{\alpha sr}$, are expressed in the form of the mass times
square of the frequency. The aerodynamic forces are
the same as those given in Ref. ([2]) and are also de-
pendent on the nodal diameter. Nondimensionalizing
Eq. (2) results in

$$\begin{bmatrix} \mu_s & x_{\alpha s}\mu_s \\ x_{\alpha s}\mu_s & r_{\alpha s}^2\mu_s \end{bmatrix} \left\{ \begin{array}{c} -h_s/b \\ -\alpha_s \end{array} \right\}$$

$$+ \sum_{r=0}^{N-1} \begin{bmatrix} (1 + 2i\zeta_{hsr})\mu_s\gamma_{hsr}^2 & 0 \\ 0 & (1 + 2i\zeta_{hsr})\mu_s r_{\alpha s}^2\gamma_{\alpha sr}^2 \end{bmatrix} \cdot$$

$$\cdot \left\{ \begin{array}{c} h_{ar}/b \\ \alpha_{ar} \end{array} \right\} e^{\frac{2\pi irs}{N}} = \sum_{r=0}^{N-1} \begin{bmatrix} l_{hhr} & l_{h\alpha r} \\ l_{\alpha hr} & l_{\alpha\alpha r} \end{bmatrix} \left\{ \begin{array}{c} h_{ar}/b \\ \alpha_{ar} \end{array} \right\}$$

$$\cdot e^{\frac{2\pi irs}{N}} + \sum_{r=0}^{N-1} \left\{ \begin{array}{c} l_{whr} \\ l_{war} \end{array} \right\} e^{\frac{2\pi irs}{N}} \qquad (3)$$

where

$$\gamma_{hsr} = \omega_{hsr}/\omega_0$$

$$\gamma_{asr} = \omega_{asr}/\omega_0 \tag{4}$$

$$\gamma = (\omega_0/\omega)^2$$

The other nondimensional variables are defined in the nomenclature and described in Ref. ($\underline{1}$). Writing these equations for all blades and arranging them in matrix form results in

$$[D]\{X\} + \gamma[Q]\{Y\} = [G][E][A]\{Y\} + [G][E]\{AD\} \tag{5}$$

where

$$[D] = \begin{bmatrix} [D_0] & & & & \\ & [D_1] & & & \\ & & \cdot & & \\ & & & \cdot & \\ & & & & \cdot \\ & & & & & [D_{N-1}] \end{bmatrix}$$

$$[D_s] = \mu_s \begin{bmatrix} 1/G_{KhsO} & x_{as}/G_{KhsO} \\ x_{as}/G_{KasO} & r^2_{as}/G_{KasO} \end{bmatrix}$$

$$G_{Khsr} = \mu_s \gamma^2_{hsr}(1 + 2i\zeta_{hsr})$$

$$G_{Kasr} = \mu_s r^2_{as}\gamma^2_{asr}(1 + 2i\zeta_{asr}) \tag{6}$$

$$[G] = \begin{bmatrix} [G_0] & & & & \\ & [G_1] & & & \\ & & \cdot & & \\ & & & \cdot & \\ & & & & \cdot \\ & & & & & [G_{N-1}] \end{bmatrix}$$

$$[G_s] = \begin{bmatrix} 1/G_{KhsO} & 0 \\ 0 & 1/G_{KasO} \end{bmatrix}$$

and

$$[Q] =$$

$$\begin{bmatrix} 1 & 0 & \frac{(1+2i\zeta_{h01})\gamma^2_{h01}}{(1+2i\zeta_{h00})\gamma^2_{h00}}E(0,1) & 0 & \frac{(1+2i\zeta_{h02})\gamma^2_{h02}}{(1+2i\zeta_{h00})\gamma^2_{h00}}E(0,2) & \cdots \\ 0 & 1 & 0 & \frac{(1+2i\zeta_{a01})\gamma^2_{a01}}{(1+2i\zeta_{a00})\gamma^2_{a00}}E(0,1) & 0 & \cdots \\ 1 & 0 & \frac{(1+2i\zeta_{h11})\gamma^2_{h11}}{(1+2i\zeta_{h10})\gamma^2_{h10}}E(1,1) & 0 & \frac{(1+2i\zeta_{h12})\gamma^2_{h12}}{(1+2i\zeta_{h10})\gamma^2_{h10}}E(1,2) & \cdots \\ 0 & 1 & 0 & \frac{(1+2i\zeta_{a11})\gamma^2_{a11}}{(1+2i\zeta_{a10})\gamma^2_{a10}}E(1,1) & 0 & \cdots \\ \vdots & \vdots & \vdots & \vdots & \vdots & \end{bmatrix}$$

The complex stiffness and mass matrices are represented by [G] and [D], respectively. The {X} and {Y} vectors represent the physical blade displacements and the modal displacements, respectively. The [E], [A], and {AD} matrices are defined in Ref. ($\underline{2}$) and are not repeated here for brevity. Using the relationship

$$\{X\} = [E]\{Y\} \tag{8}$$

to remove the physical blade displacements from the system of equations results in

$$[P]\{Y\} = \gamma[Q]\{Y\} - [G][E]\{AD\} \tag{9}$$

where

$$[P] = [G][E][A] + [D][E] \tag{10}$$

The aeroelastic stability of the system, can be determined from the eigenvalues, γ's, of the generalized problem

$$\big[[P] - \gamma[Q]\big]\{Y\} = 0 \tag{11}$$

The relation between the eigenvalue, γ, and the complex frequency is

$$\frac{i\omega}{\omega_0} = \frac{1}{\sqrt{\gamma}} = \bar{\mu} + i\bar{v} \tag{12}$$

Therefore, $\bar{\mu}$ is a measure of the damping or stability of the mode and $\bar{v}$ is a measure of the frequency. For the discussion of results to follow, a mode is considered to be stabilized when $\bar{\mu}$ becomes more negative and destabilized when it becomes more positive. The aeroelastic response can be derived from Eq. (9) and is

$$\{Y\} = \big[\gamma[Q] - [P]\big]^{-1}[G][E]\{AD\} \tag{13}$$

II. RESULTS AND DISCUSSION

A computer program was written to calculate the stability and response of a mistuned bladed-disc including both aerodynamic and structural coupling of the blades using the formulation presented in the last section. In this program it is possible to consider arbitrary mistuning of the blade uncoupled bending and torsional frequencies and damping coefficients. The quantities γ_{hsr} and γ_{asr}, see Eq.(4), must be supplied as input to this formulation. The approach used herein is to calculate the frequencies of the tuned rotor for each nodal diameter up to N/2 (N/2-1 for an odd number of blades).

4

$$\gamma_{hr} = \omega_{hr}/\omega_0 = \gamma_{hN-r}$$

$$\gamma_{ar} = \omega_{ar}/\omega_0 = \gamma_{aN-r}$$

(14)

For example, for a 24 bladed rotor in vacuum the frequency of the $r = 5$ mode is the same as that of the $r = 19$ mode since the structural properties cannot distinguish between a forward and backward traveling wave of the same nodal diameter. There are a number of methods available to calculate the quantities γ_{hsr} and γ_{asr}; the most general being the finite element method. However, it is sufficient for the purposes of this paper to assume that the mistuned system frequencies are given by

$$\gamma_{hsr} = \gamma_{hr}(\omega_{hs}/\omega_0)$$

$$\gamma_{asr} = \gamma_{ar}(\omega_{as}/\omega_0)$$

(15)

in which ω_{hs} and ω_{as} are the blade alone frequencies. This has been shown in Ref. (22) to be a valid assumption for small deviations in ω_{hs} and ω_{as} when the bladed-disc motion is blade dominated. In the following sections two different rotors are analyzed: (1) a twelve bladed rotor representative of a set of blades connected by midspan shrouds (considered in Ref. (4)) and (2) a more realistic unshrouded bladed disk representative of an advanced fan stage. Both alternating and random torsional frequency mistuning are considered. Since the effects of bending-torsion coupling were examined in Refs. (1) and (2), the emphasis in this paper is on the torsional motion. As a result the predominantly bending modes are not shown in the results to follow.

A. Flutter

To provide a check for a special case of the present formulation and computer code, an aeroelastic stability analysis is conducted for a tuned rotor with 12 blades which was considered in Ref. (4). The blades have significant structural coupling due to the presence of midspan shrouds. In addition to providing a check, the results give an example of the effect of structural coupling due to midspan shrouds on the system eigenvalues. The formulation in Ref. (4) includes only single degree-of-freedom torsional blade motion. As a result, the bending frequencies in the present formulation are set to 10 times the torsional frequencies. This minimizes the inertial coupling between the bending and torsional motions and provides a direct comparison with Ref. (4) results. The parameters of interest for this rotor are given in Table I. The dependency of blade torsional frequencies on nodal diameter as taken from Ref. (4) is given in Table II for the reader's convenience. Figure 2 presents the eigenvalues for two cases of the tuned system; (1) no structural coupling and where the uncoupled blade torsional frequencies are equal to ω_0 and (2) a flexible shroud ring in which the the frequency dependence is given in Table II. In this figure the plus symbol represents the eigenvalue for the case in which there is no structural coupling. The number adjacent to the symbol gives the predominant interblade angle for that eigenvalue. The arrow represents the location to which the eigenvalue moves (the end of the arrowhead) when the effects of structural coupling are considered. Note that for some modes the movement is so small that the arrows are not drawn. Within plotting accuracy, the results obtained using the present formulation are identical to those of Fig. 6 in Ref. (4). Note that there are different eigenvalue definitions between this

paper and the reference. Since $\bar{\mu}$ only changes slightly, the addition of structural coupling has little effect on the stability of the individual modes. As expected, for certain modes the frequency is significantly affected. As was stated in Ref. (4), it is believed that this behavior is representative of shrouded blades when the shroud ring is relatively stiff compared to the blades.

To determine the effects of structural coupling on the coupling between the interblade phase angle modes in the presence of mistuning, this rotor was analyzed with 5 percent alternating mistuning. With this type of mistuning the torsional frequency alternates from blade to blade as you proceed around the disk. All odd numbered blades would have the identical frequency and all even numbered blades have the same frequency. The percent mistuning being defined as the difference in these two frequencies divided by the average. The resulting eigenvalues both with and without structural coupling are given in Fig. 3. The structural coupling generally only affects the frequency of the modes. However, it is interesting to note that the predominantly 60 degree interblade phase angle mode (2 nodal diameter) is somewhat destabilized.

To determine the effects of structural coupling on a more realistic rotor, an advanced fan stage called Rotor I is now analyzed. The parameters of this rotor are given in Table I. The assumed dependency of the tuned torsional frequencies (in vacuum) versus the nodal diameter is shown in Fig. 4. This assumption is based on previous experience using finite element techniques to predict the natural frequencies of similar bladed-discs. Figure 5 shows the effect of the structural coupling on the tuned system. As in the previous case, the effect is to significantly change the frequency of certain modes with little effect on the stability. This behavior is to be expected since each of the nodal diameter modes is uncoupled from the others. Note that there are still a number of unstable modes.

Rotor I is now analyzed with the assumption of alternate mistuning. As seen in Fig. 6, all of the modes of Rotor I are stable in the presence of 10 percent alternating mistuning without structural coupling. However, certain modes are significantly destabilized by the inclusion of structural coupling. Although all of the modes are stable, this behavior could result in a significant increase in aeroelastic response since the effective damping is decreased.

Random mistuning is now considered. Using the blade frequency distribution shown in Fig. 7 (mean of 1.001 and standard deviation of 0.034, a typical production distribution) the eigenvectors of Rotor I without structural coupling were calculated and are displayed in Fig. 8. The analysis was repeated including the effects of structural coupling and the corresponding results are shown in Fig. 9. Comparing Figs. 8 and 9, it is seen that both the frequency and stability of the modes is significantly affected. It is important to note that the predominantly 45 degree interblade phase angle mode is moved into the unstable region. Although not shown, the blade amplitude distributions for most of the modes are drastically different when comparing the results with and without structural coupling.

B. Aeroelastic Response

In the present formulation it is possible to consider an excitation from symmetrically spaced obstructions located upstream from the blades. The number of obstructions is known as the engine order of the excitation and is usually represented by an integer fol-

lowed by "E". For example, 5E would represent a perfectly sinusoidal excitation resulting from 5 upstream obstructions. For a more detailed description of the formulation of the aeroelastic response problem see Refs. (1) and (2).

To illustrate the affect of structural coupling on response, Rotor I is again analyzed with the torsional frequency dependency shown in Fig. 4. The 5E resonance is investigated for the tuned, 10 percent alternating mistuned, and randomly mistuned conditions. The Mach number is 0.8 and the reduced frequency is 0.6. All other parameters are the same as those given in Table I. These parameters were chosen so that all modes of the rotor are stable in the tuned condition.

The eigenvalues for the tuned condition including structural coupling are shown in Fig. 10. The movement of the eigenvalue of interest (-56 degrees interblade phase angle or 5 nodal diameter backward traveling wave) is represented by the arrow in Fig. 10. That is, the tail of the vector represents the position of the eigenvalue without structural coupling. The resonance peaks both with and without structural coupling are shown in Fig. 11. As expected, the frequency at which the rotor has maximum amplitude is approximately 4 percent lower with structural coupling. In addition, the maximum amplitudes are approximately equal.

The eigenvalues for the system with 10 percent alternating mistuning are shown in Fig. 12. For this type of mistuning the 5E forcing function can excite only the -56 and 123 degree interblade phase angle modes. The movement of these modes, depicted by the arrows in Fig. 12, represents primarily a change in frequency. As is the case for alternate mistuning, the single resonance peak is replaced by twin peaks which are shown in Fig. 13. Although not shown, the curves without structural coupling have the same general shapes and amplitudes with only shifts in frequency.

The final case to be investigated is that of random mistuning. The in vacuum frequency distribution of Fig. 7 is again used. The system eigenvalues are shown in Fig. 14. Comparing these eigenvalues with those without structural coupling (not shown), it is found that both the frequency and stability of certain modes was significantly affected. However, since the 5E forcing function excites all of the interblade phase angle modes in this case, it is difficult to predict whether the amplitude of response will be larger or smaller than those of the rotor with no structural coupling. The response curve with multiple resonance peaks is shown Fig. 15. As expected, blade 2 has the maximum response at low forcing frequencies and blade 17 has the maximum response at high forcing frequencies. Comparing this curve with that for no structural coupling (not shown), it was found that the inclusion of structural coupling had not significantly changed the overall response amplitudes. However, the blade-to-blade amplitude distributions have changed somewhat. For example, blades 10 and 14 have the highest amplitudes when the forcing frequency is approximately in the range 1 to 1.05. When there was no structural coupling, blades 3 and 13 were found to have the maximum amplitude in this forcing frequency range.

III. CONCLUSIONS

The analyses of the effects of mistuning on coupled bending torsion flutter and response which were developed in Refs. (1) and (2) have been extended to include the effects of structural coupling between the blades. The following conclusions are reached based on the parametric studies presented herein for bladed-discs in which the motion is dominated by the blades.

1. The addition of structural coupling can affect both the frequency and aeroelastic stability.

2. The stability is significantly affected only when the system is mistuned. The affect can be either beneficial or detrimental depending on the type of mistuning, the type of structural coupling, and the cascade parameters.

3. The resonant frequencies can be significantly affected by structural coupling in both tuned and mistuned systems, however, the peak response is significantly affected only for the latter.

REFERENCES

1. Kaza, K. R. V. and Kielb, R. E., "Flutter and Response of a Mistuned Cascade in Incompressible Flow," AIAA Journal, (Vol. 20, No. 8) Aug. 1982, pp. 1120-1127.

2. Kielb, R. E. and Kaza, K. R. V., "Aeroelastic Characteristics of Cascade of Mistuned Blades in Subsonic and Supersonic Flows," ASME Paper No. 81-DET-122, Sept. 1981.

3. Kielb, R. E., "Aeroelastic Characteristics of a Mistuned Bladed-Disc Assembly," Ph.D. Dissertation, The Ohio State University, Columbus, Ohio, 1981.

4. Srinivasan, A. V., "Influence of Mistuning on Blade Torsional Flutter," R80-914545-16, United Technologies Research Center, East Hartford, Conn., Aug. 1980. (NASA CR-165137)

5. Smith, S. N., "Discrete Frequency Sound Generation in Axial Flow Turbomachines, "A. R. C. R&M No. 3709, 1973.

6. Adamczyk, J. J. and Goldstein, M. E., "Unsteady Flow in a Supersonic Cascade with Subsonic Leading-Edge Locus," AIAA Journal, Vol. 16, No. 12, Dec. 1978, pp. 1248-1254.

7. Wagner, J. T., "Coupling of Turbomachine Blade Vibrations Through the Rotor," ASME Journal of Engineering for Power, Vol. 89, No. 4, Oct. 1967, pp. 502-512.

8. Dye, R. C. F. and Henry, T. A., "Vibration Amplitudes of Compressor Blades Resulting from Scatter in Blade Natural Frequencies," ASME Journal of Engineering for Power, Vol. 91, No. 3, July 1969, pp. 182-188.

9. Ewins, D. J., "Bladed Disc Vibration - A Review of Techniques and Characteristics," Recent Advances in Structural Dynamics, Vol. 1, M. Petyt, ed., University of Southampton, Southampton, England, 1980, pp. 187-210.

10. El-Bayoumy, L. E. and Srinivasan, A. V., "Influence of Mistuning on Rotor-Blade Vibrations," AIAA Journal, Vol. 13, No. 4, Apr. 1975, pp. 460-464.

11. Whitehead, D. S., "Effect of Mistuning on the Vibration of Turbomachine Blades Induced by Wakes," Journal of Mechanical Engineering and Science, Vol. 8, No. 1, Mar. 1966, pp. 15-21.

12. Whitehead, D. S., "Torsional Flutter of Unstalled Cascade Blades at Zero Deflections," ARC R and M-3429, 1964.

13. Hanamura, Y. and Tanaka, H., "A Modification of Flutter Characteristics by Changing Elastic Nature of Neighboring Blades in Cascades," Tokyo Joint Gas Turbine Congress, Gas Turbine Society of Japan, Tokyo, 1977, pp. 418-425.

14. Ford, R. A. J. and Foord, C. A., "An analysis of Aeroengine Fan Flutter Using Twin Orthogonal Vibration Modes," ASME Paper 79-GT-126, Mar. 1979.

15. Hanamura, H., "Flutter of Cascading Blade Row," Institute of Space and Aeronautical Science, University of Tokyo, Vol. 36, No. 1, Report No. 459, 1971, pp. 1-36.

16. Shiori, J., "Non-Stall Normal Mode Flutter in Annular Cascades, Part II-Experimental Study," Transactions of Japan Society of Aeronautical Engineering, Vol. I, No. 1, 1958, pp. 26-45.
17. Carta, F. O., "Coupled Blade-Disc-Shroud Flutter Instabilities in Turbojet Engine Rotors," ASME Journal of Engineering for Power, Vol. 89, No. 3 July 1967, pp. 419-426.
18. Rao, B. M. and Kronenburger, L., Jr., "Aeroelastic Characteristics of a Cascade of Blades," AFOSR-TR-78-1027 Texas A&M Research Foundation, College Station, Texas, Feb. 1978.

19. Bendiksen, O. and Friedmann, P., "Coupled Bending-Torsion Flutter in Cascades," AIAA Journal, Vol. 18, No. 2, Feb. 1980, pp. 194-201.
20. Dugundji, J., "Flutter Analysis of a Tuned Rotor with Rigid and Flexible Disks," GT&PDL Report No. 146, M. I. T., Cambridge, Mass. July 1979.
21. Kaza, K. R. V. and Kielb, R. E., "Coupled Bending-Bending-Torsion Flutter of a Mistuned Cascade With Nonuniform Blades," AIAA Paper 82-0726, 1982.
22. Crawley, E. F., Massachusetts Institute of Technology, "Private Communication" on Stiffness Matrix Perturbations."

TABLE I. - ROTOR PARAMETERS

Parameter	Symbol	Ref. (4) rotor	Rotor I
Reduced frequency	k	0.75	0.441
Number of blades	N	12	32
Stagger angle	ξ	60°	62°
Elastic axis position	a	0.2	0
Gap-to-chord ratio	s/c	0.8	0.777
Mass ratio	μ_s	73.9	141
Radius of gyration	r_{α_s}	0.611	0.47
Elastic axis-C.G. offset	x_{α_s}	-0.2	0
Mach number	M	0.84	1.18
Bending to torsion frequency ratio tuned	$\omega_{hs}/\omega_{\alpha s}$	10	0.3

TABLE II. - FREQUENCY

DISTRIBUTION

(IN VACUUM)

r	$\gamma_{\alpha r}$
0	1.0000
1 and 11	.99928
2 and 10	.99724
3 and 9	.98396
4 and 8	1.0027
5 and 7	1.0004
6	1.0000
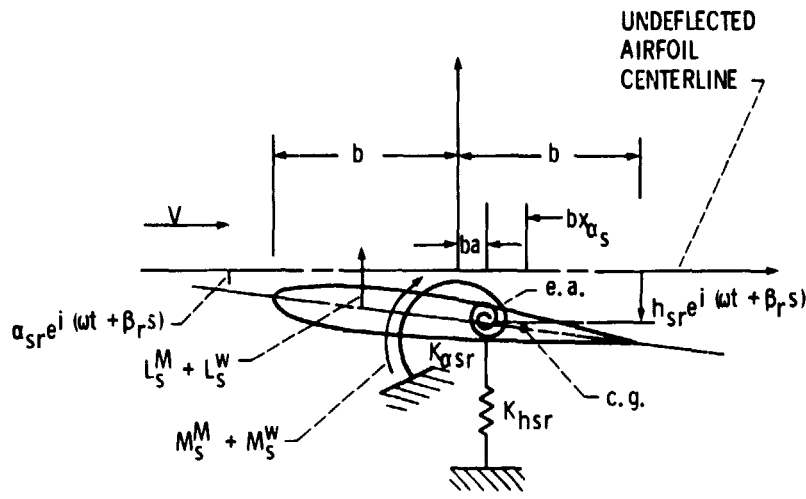
e.a. - ELASTIC AXIS
c.g. - CENTER OF GRAVITY

Figure 1. - Typical section model.
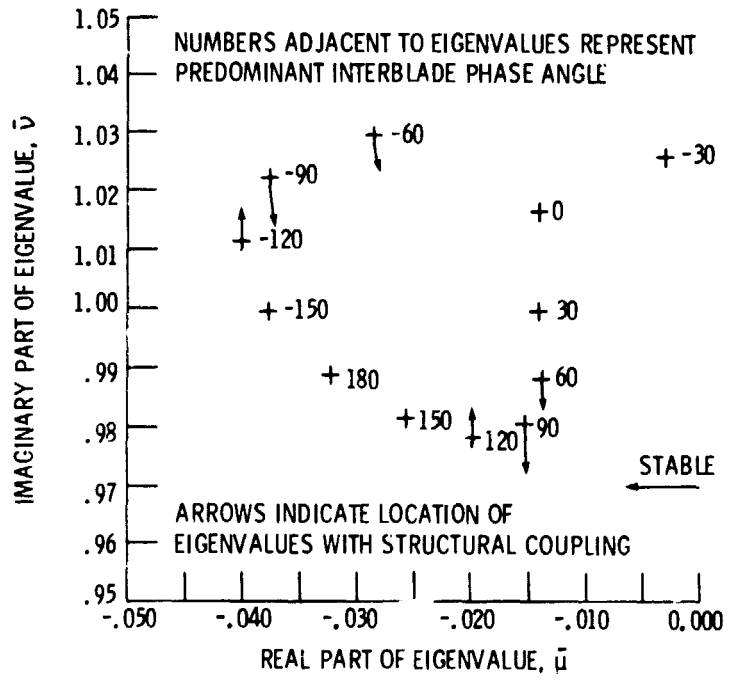
Figure 2. - Eigenvalues of rotor with 12 blades (tuned),
M = 0.84
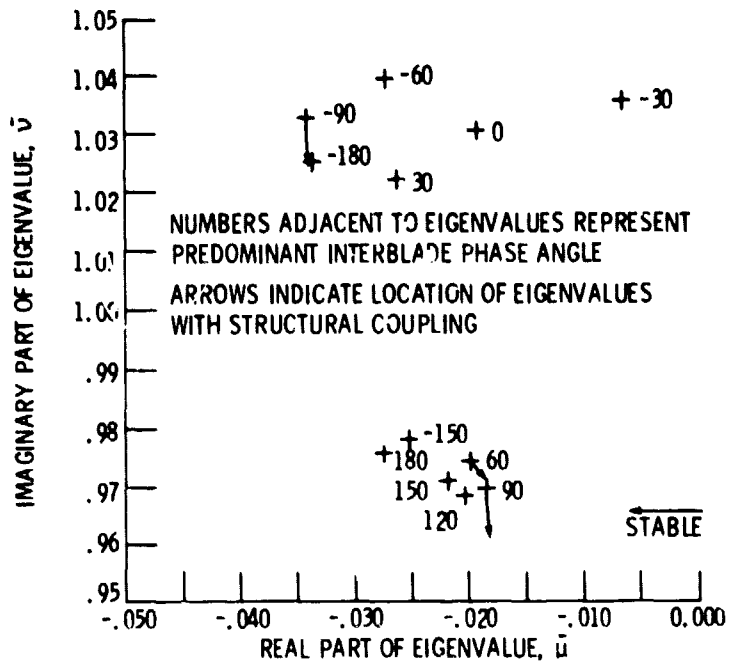
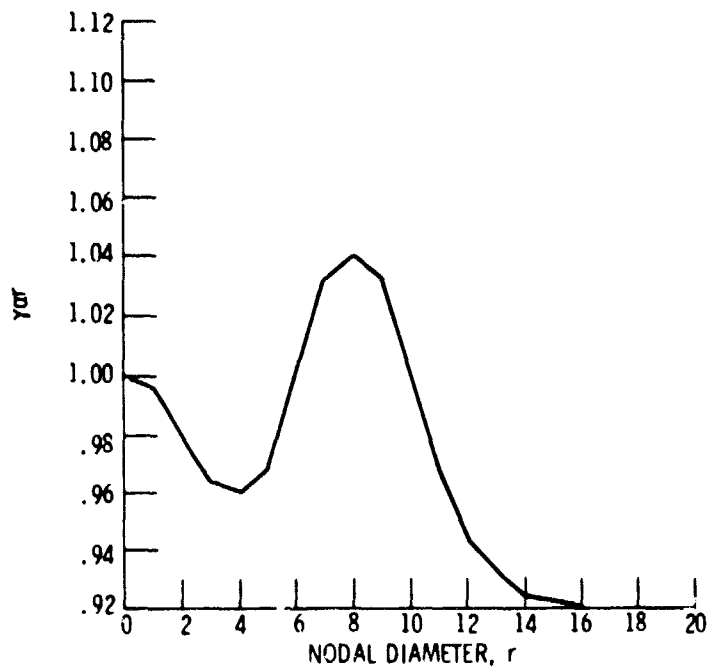Figure 3. - Eigenvalues of rotor with 12 blades (5% alternating mistuning), M = 0.84.

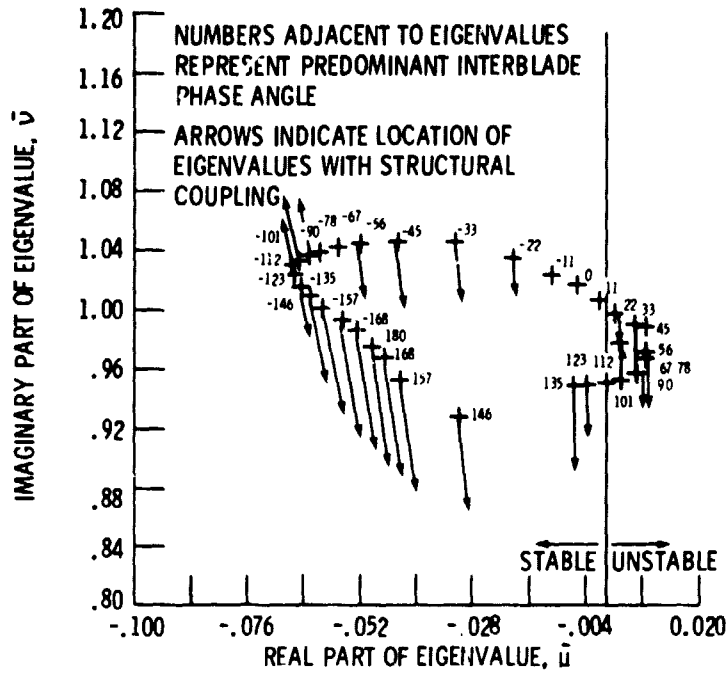Figure 4. - Assumed frequency distribution of rotor I (in vacuum).
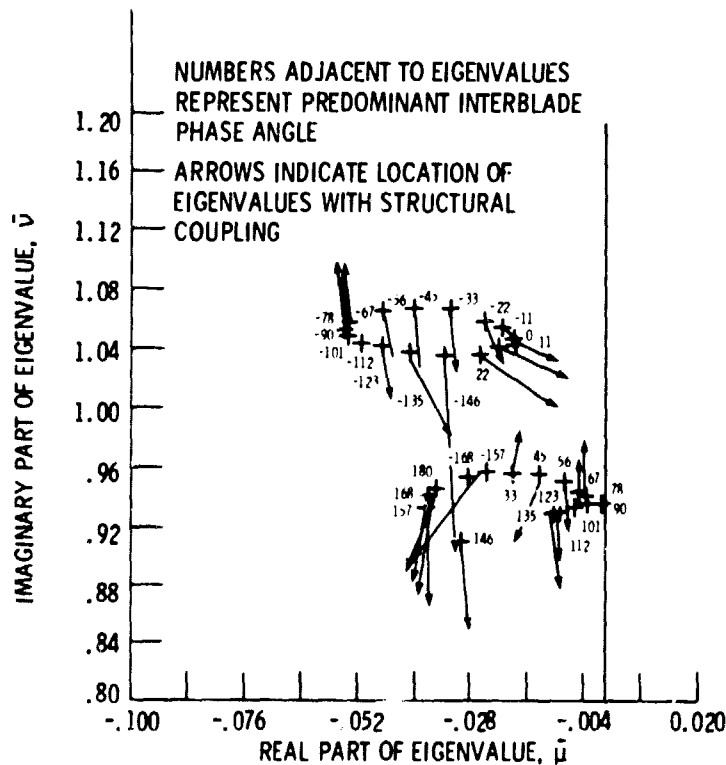
Figure 5. - Eigenvalues of rotor I (tuned), M = 1.18.

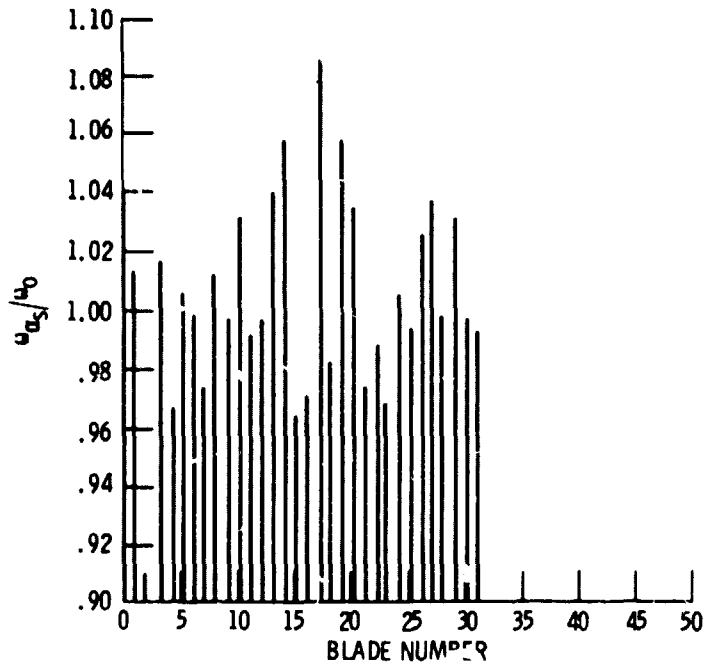Figure 6. - Eigenvalues of rotor I (10% alternating mistuning), M = 1.18.

Figure 7. - Random torsional frequency distribution.
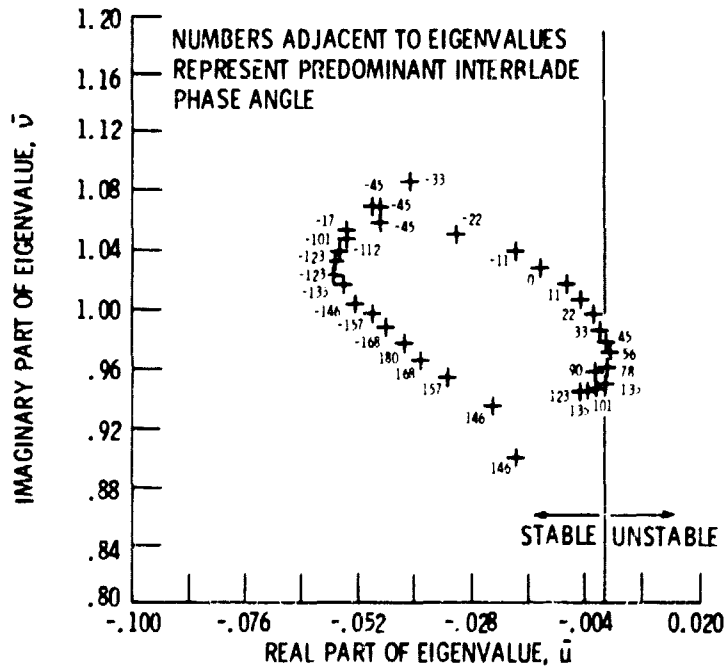
Figure 8. - Eigenvalues of rotor I, no structural coupling (random mistuning), M = 1.18.
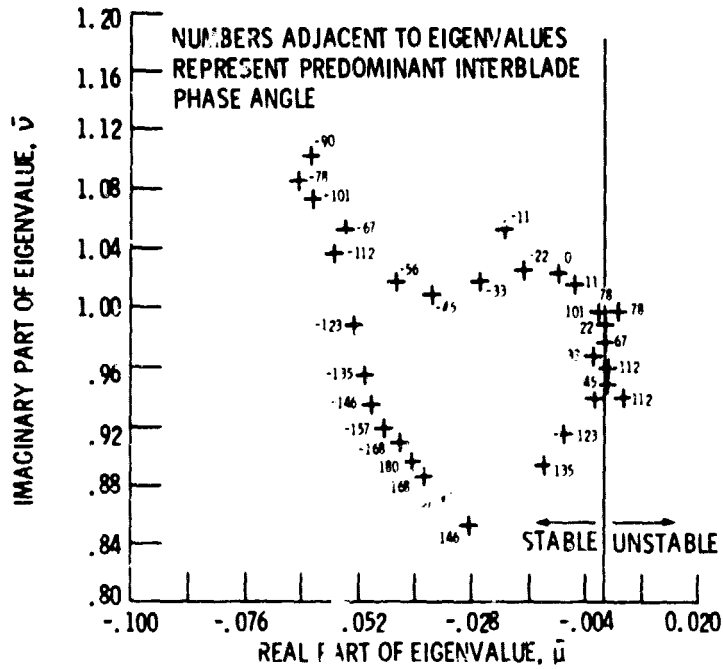
Figure 9. - Eigenvalues of rotor I, with structural coupling (random mistuning), M = 1.18.
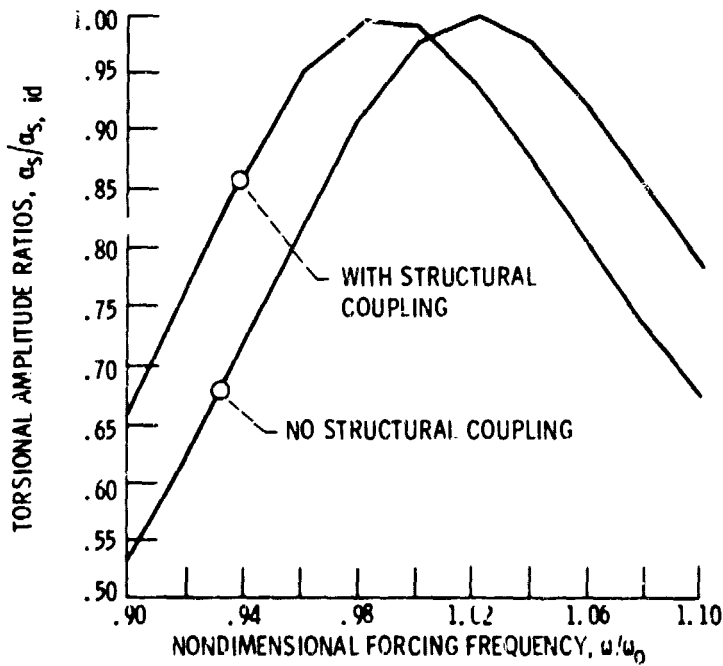
Figure 10 - Tuned 5E response of rotor I, M = 0.8.
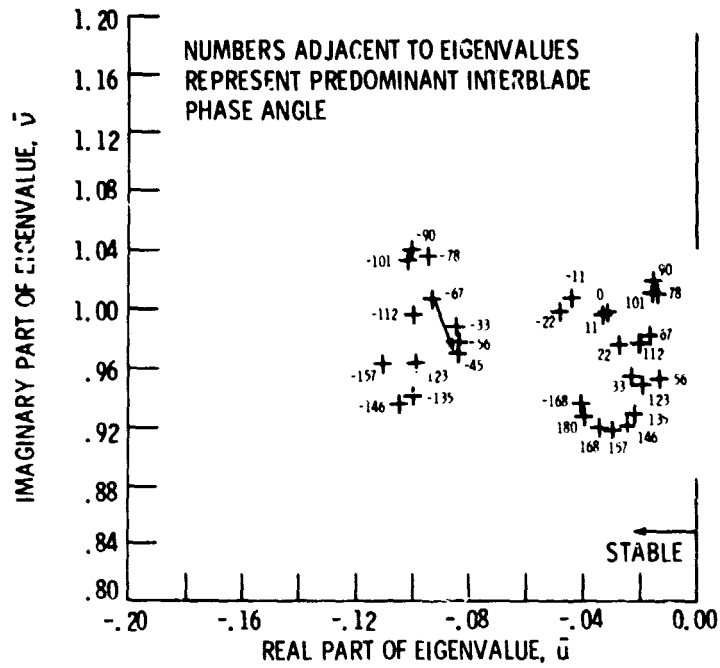
Figure 11. - Tuned 5E response of rotor I, M = 0.8.
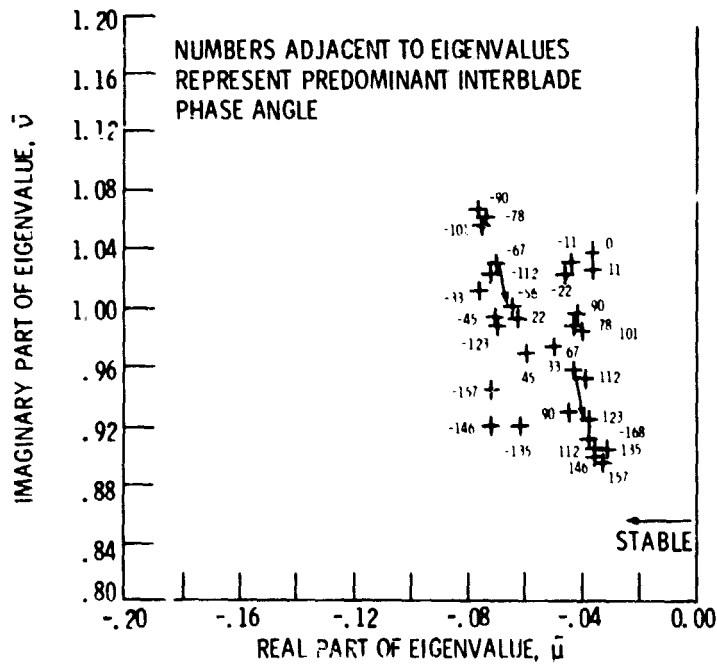
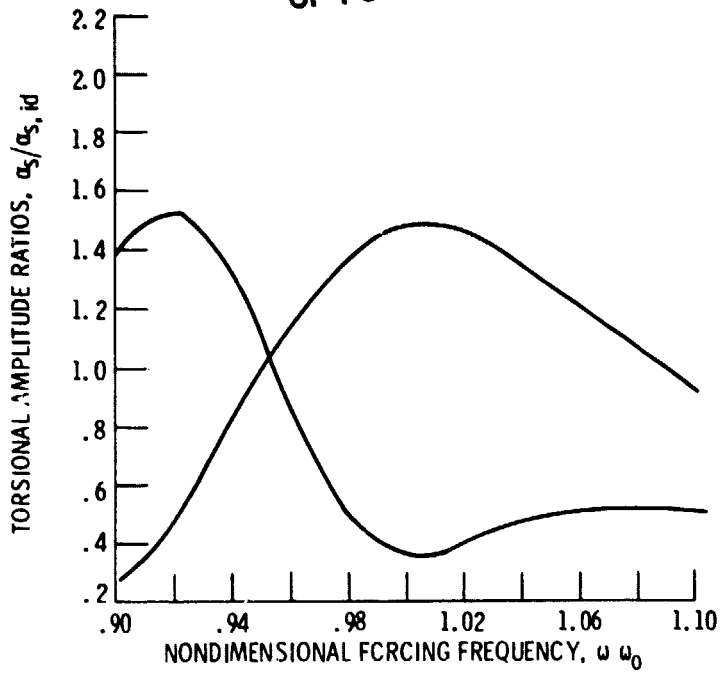Figure 12. - Eigenvalues of rotor I, M = 0.8 (10% alternating mistuning).

Figure 13. - 5E response of rotor I with 10% alternating mistuning, M = 0.8.
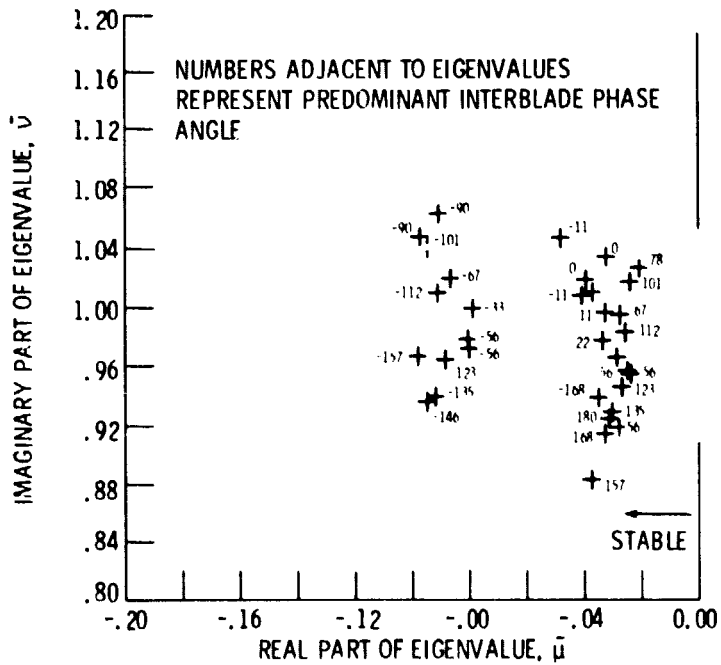

NUMBERS ADJACENT TO EIGENVALUES
REPRESENT PREDOMINANT INTERBLADE PHASE
ANGLE

STABLE

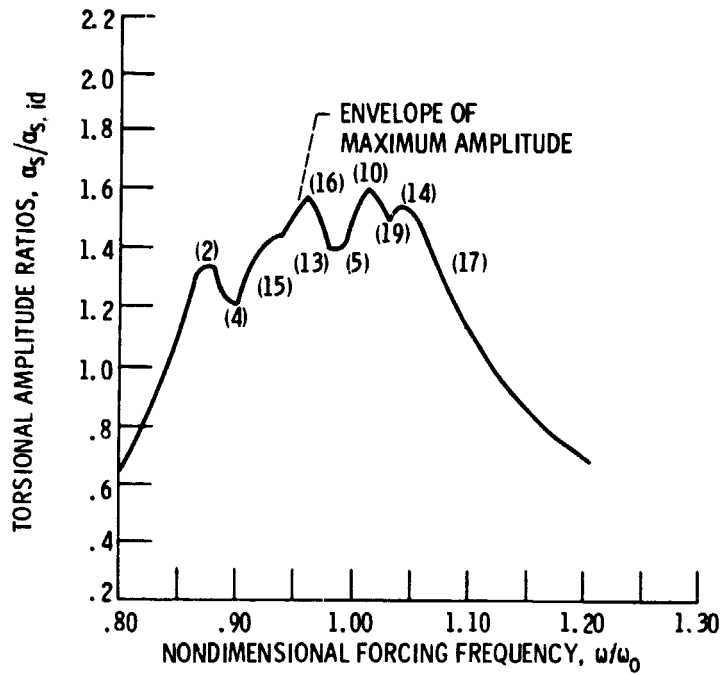Figure 14. - Eigenvalues of rotor I, M = 0.8 (Random mistuning).

Figure 15. - 5E response of rotor I with random mistuning, M = 0.8.